Radar: Generation of a Displacement Map

Timothy Simons — s1116752

December 19, 2025

Abstract

This project uses Sentinel-1 Interferometric Synthetic Aperture Radar (InSAR) to measure surface deformation caused by the Ridgecrest earthquake in July 2019. Two SAR images were processed with SNAP and SNAPHU to produce displacement results, which show displacement across the Garlock fault line exceeding one metre.

Contents

1 Introduction

The study area for this project is the M_w 7.1 Ridgecrest earthquake that occurred on 5th July 2019 in California, U.S. This earthquake was caused by a slippage of tectonic plates along the Garlock Fault in the Little Lake fault zone [5] [6]. Radar interferometry is the perfect candidate for analysing such an event.

Interferometric Synthetic Aperture Radar (InSAR) can effectively detect and measure deformation of the earth's crust. Sentinel-1A, with a repeat cycle of 12 days, captured SAR images of the target area before and after the event. These SAR images can be compared to produce an interferogram, which contains information about the resulting displacement in the earth's surface caused by this earthquake.

2 Methods

2.1 Data Acquisition

The Corpernicus browser was used to acquire the two SAR images used for InSAR analysis. The satellite captured the data in Interferometric Wide (IW) mode, which easily includes the target area in its 250km swath.

The SLC product is used as it retains phase information necessary to perform InSAR. The relative orbit number defines which ground track is being used and the orbit direction affects the viewing geometries of the satellites; both should be kept constant between the two images.

The sensing time of the two images are very close to one another (exactly 12 days apart). This short temporal baseline helps reduce a phenomena known as temporal de-correlation, which ensures the resulting interferogram has high coherence.

Attribute	**Image 1**	**Image 2**
Product name	S1A_IW_SLC_1SDV_20190704	S1A_IW_SLC_1SDV_20190716
Sensing time (UTC)	2019-07-04 13:51:58	2019-07-16 13:51:59
Platform	Sentinel-1A	Sentinel-1A
Instrument	SAR	SAR
Processing level	Level-1	Level-1
Product type	SLC	SLC
Operational mode	IW	IW
Relative orbit number	71	71
Absolute orbit number	27,968	28,143
Orbit direction	Descending	Descending
Polarisation	VV, VH	VV, VH
Swaths	IW1, IW2, IW3	IW1, IW2, IW3

Table 1: Summary of Sentinel-1 SAR images used for InSAR analysis of the Ridgecrest earthquake.

2.2 Data Preparation

2.2.1 Load Sentinel-1 Images

The two SAR images were loaded into SNAP. Each product contains 3 subswaths and 9 bursts per subswath. The bands include complex (I and Q) magnitude values [4] and polarisations VV, VH.

2.2.2 Split the Subswath

See Figure 10.

The IW-2 subswath and bursts 4-6 were selected for both SAR images using the S-1 TOPS Split tool. The VV polarisation was selected for this analysis. This reduces the area of interest to only include the target area, which will help speed up subsequent computations.

2.2.3 Apply Orbit File

See Figure 11.

Precise Orbit Determination (POD) files were used to improve the accuracy (e.g. for geometric correction [4]) of the SAR images. The Sentinel Precise (Auto-Download) option downloads the highest accuracy POD file available. If we examine the Metadata of the resulting product, we can see that a POEORB file was used for orbit correction.

2.3 Generation of Topographic Interferogram

2.3.1 Coregistration (Back-Geocoding)

See Figure 12.

The S-1 Back-Geocoding tool was used to align the two SAR images in a process known as coregistration. It uses orbital information from the previous step and information from a digital elevation model to align the pixels in the first image with pixels in the second image.

The default SRTM (Shuttle Radar Topography Mission) 3 Arc Second DEM is used. This DEM offers a good trade-off between speed and resolution ($\sim 90m$).

2.3.2 Interferogram Formation

See Figure 13.

The Interferogram Formation computes the phase difference between the two images. The interferogram represents the difference in travel paths of the radar signal between the two SARs.

We are interested in the phase difference caused by surface deformation, and so we will subtract flat-earth phase in this step (and later we will also remove topographic phase).

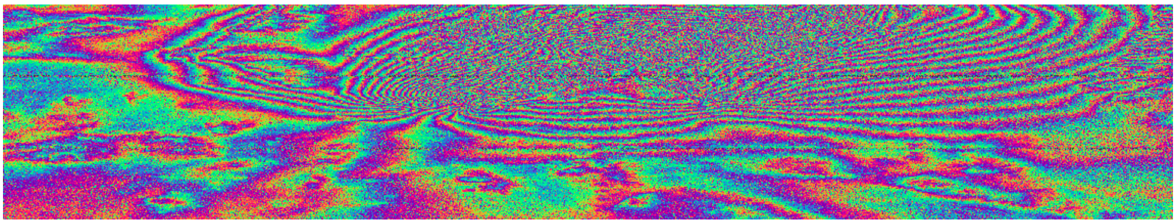

Figure 1: Interferogram

2.3.3 TOPSAR Deburst

See Figure 14.

The TOPS Deburst tool is used to remove seam-lines between bursts.

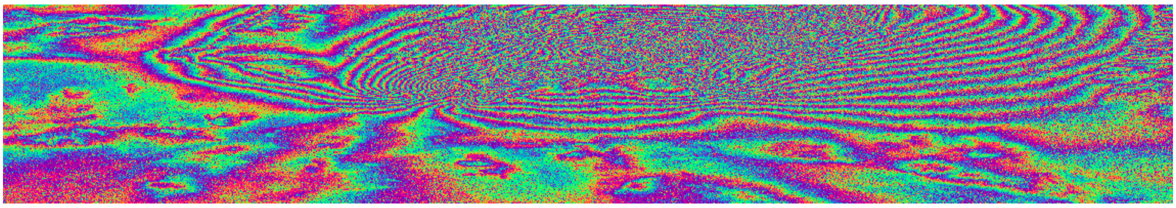

Figure 2: TOPSAR Deburst

2.4 Generation of Differential Interferogram

2.4.1 Topographic Phase Removal

See Figure 15.

After topographic phase removal, the remaining phase difference should be due to displacement, atmosphere and noise [1].

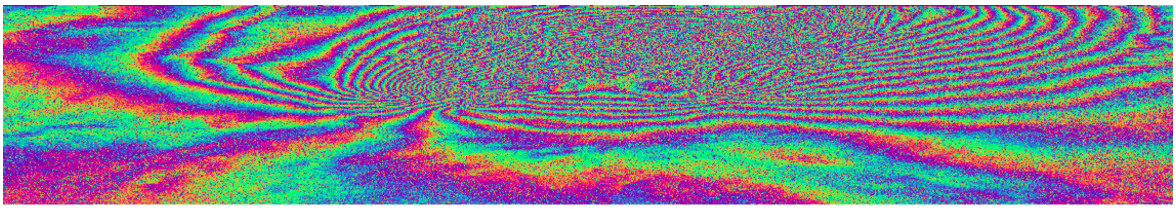

Figure 3: Topographic Phase Removal

2.4.2 Multilooking

See Figure 16.

Multilooking reduces noise and also produces a product with a nominal image pixel size [2].

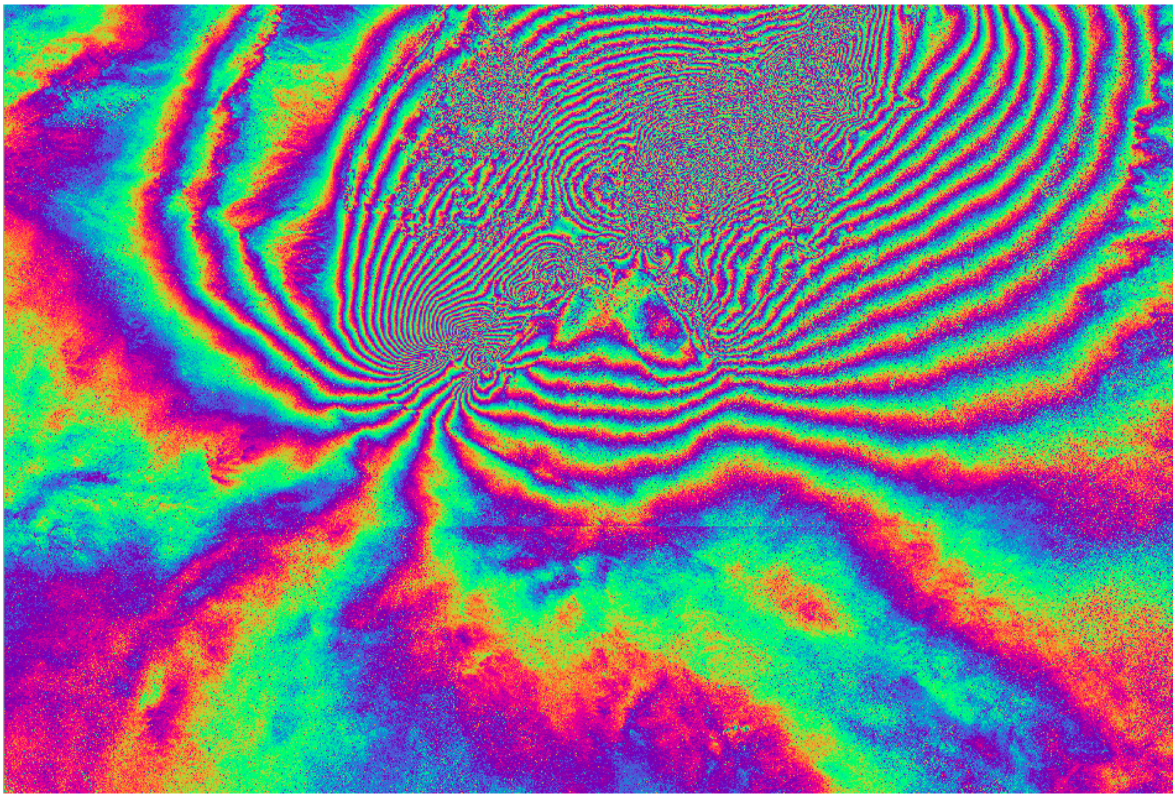

Figure 4: Multilooking

2.4.3 Goldstein Phase Filtering

See Figure 17.

Goldstein Phase Filtering further removes noise and improves the quality of fringes in the interferogram.

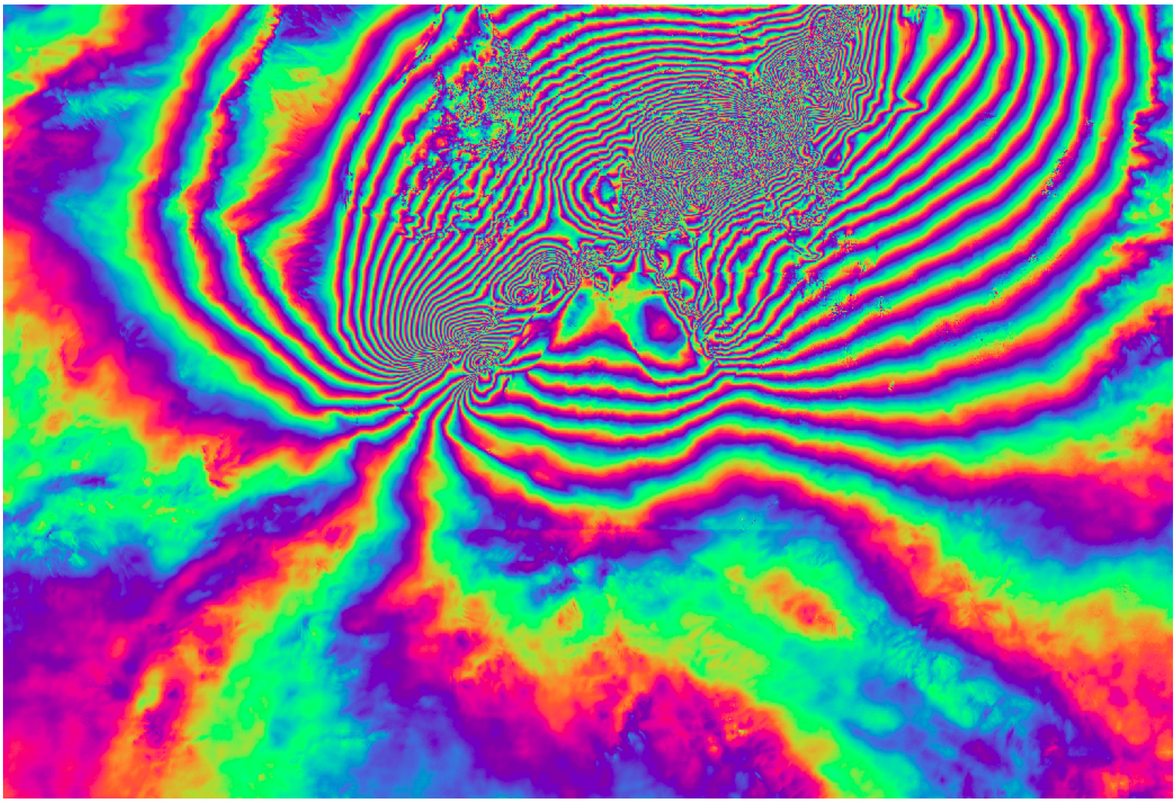

Figure 5: Goldstein Phase Filtering

2.5 Phase Unwrapping

2.5.1 SNAPHU Export

See Figure 18.

2.5.2 Run SNAPHU

Phase unwrapping removes 2π ambiguity from the interferogram. The result represents the relative height/displacement between pixels [1].

The Snaphu configuration file was modified manually to set the number of tile rows and tile columns to 1 because the default values in the Snaphu Export produced tiling errors in the resulting product.

2.5.3 SNAPHU Import

See Figure 19.

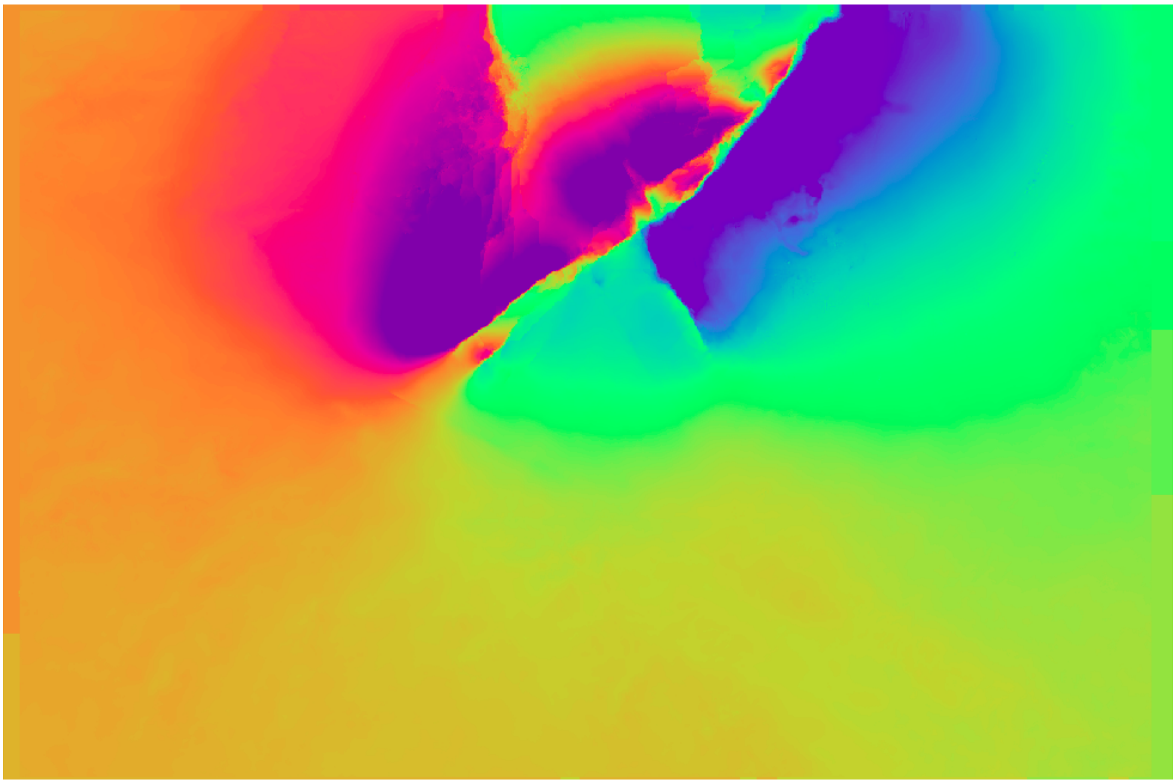

Figure 6: SNAPHU Import

2.6 Generation of Displacement Map

2.6.1 Phase to Displacement

See Figure 20.

The unwrapped phase is not a metric that we can easily understand and interpret, and so we convert it into absolute displacement values.

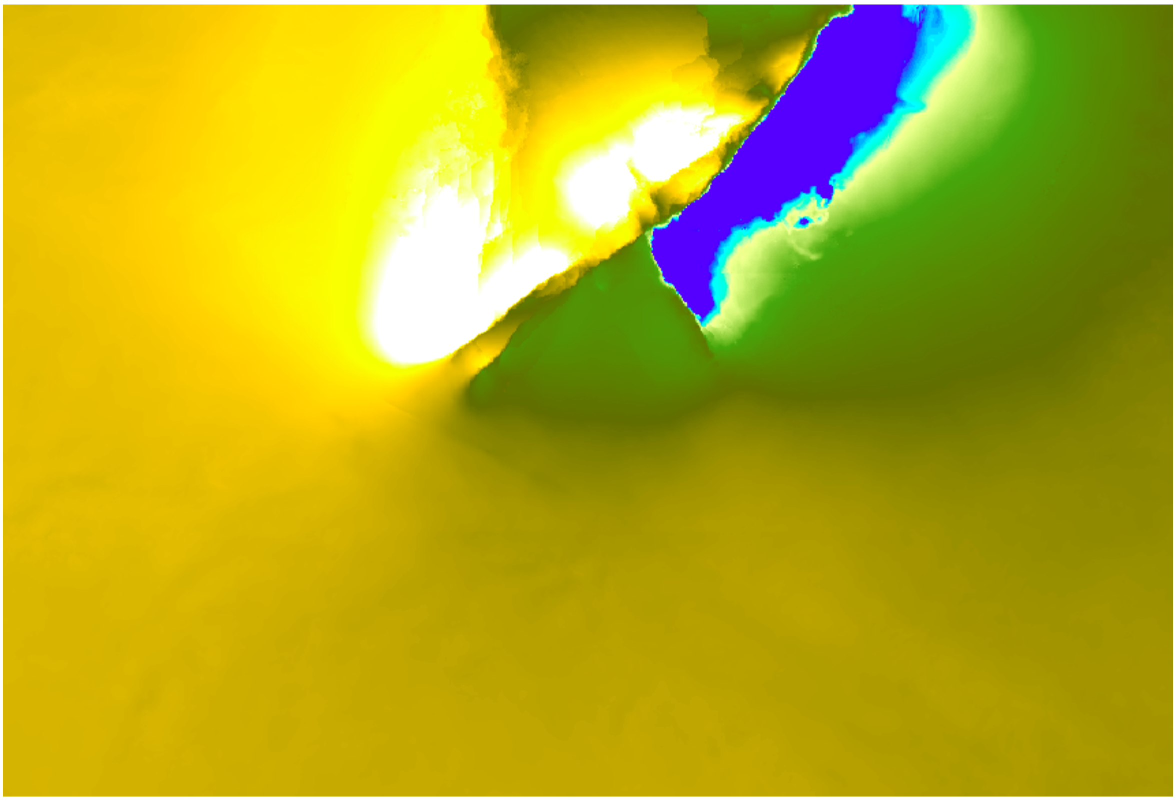

Figure 7: Phase to Displacement

2.6.2 Terrain Correction

Terrain correction projects the displacement image into a map coordinate system.

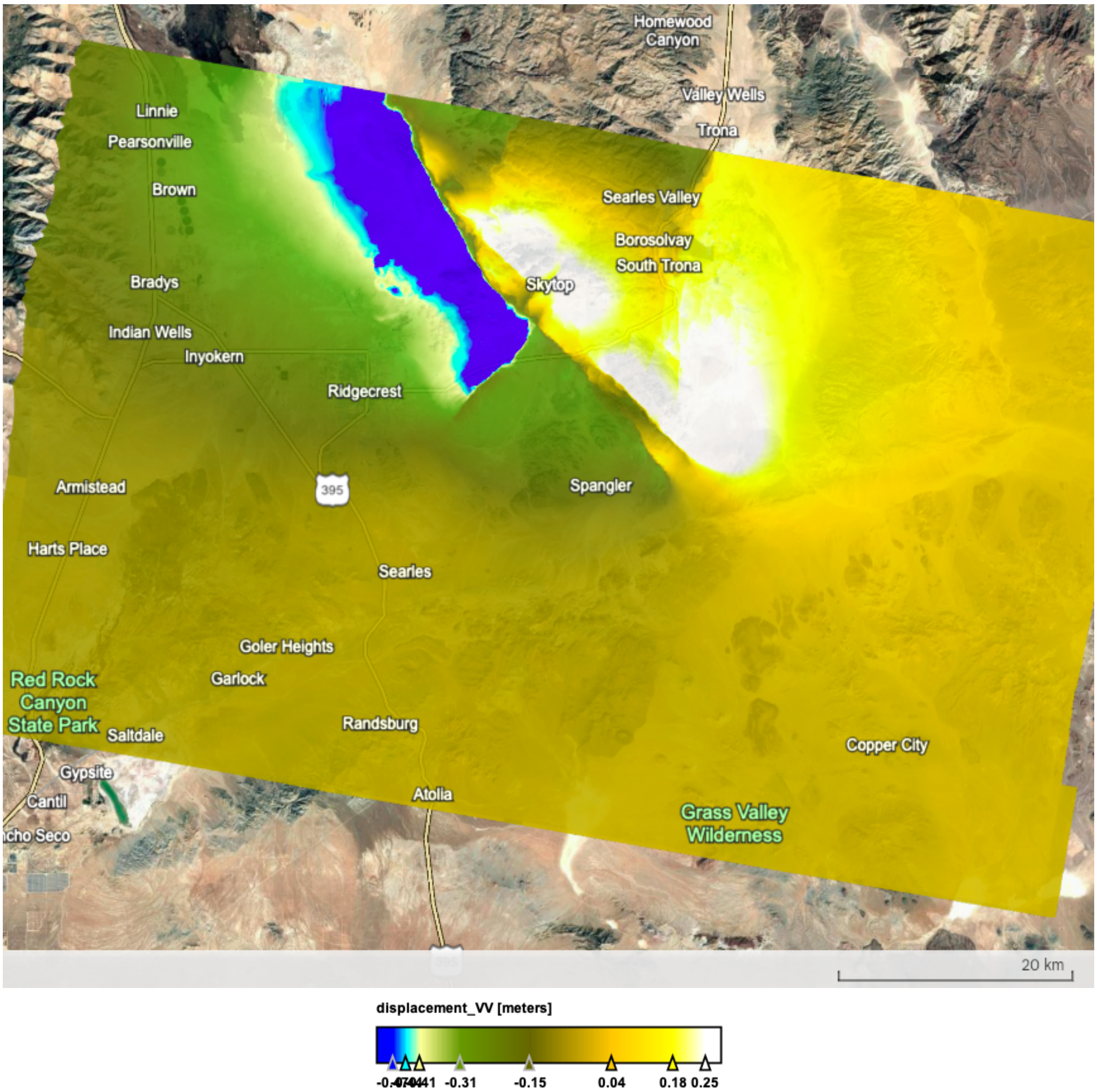

Figure 8: Terrain Correction

3 Analysis

The displacement measurements produced by this InSAR analysis showed a minimum value of -1124mm and a maximum value of +739mm.

The Profile Plot Tool can be used to visualise the change of displacement along a line. The drawn line in Figure 9 is orthogonal to the fault line. The rate of change of displacement is large when the drawn line intersects the fault. The displacement values ranges from approximately +400mm to -400mm.

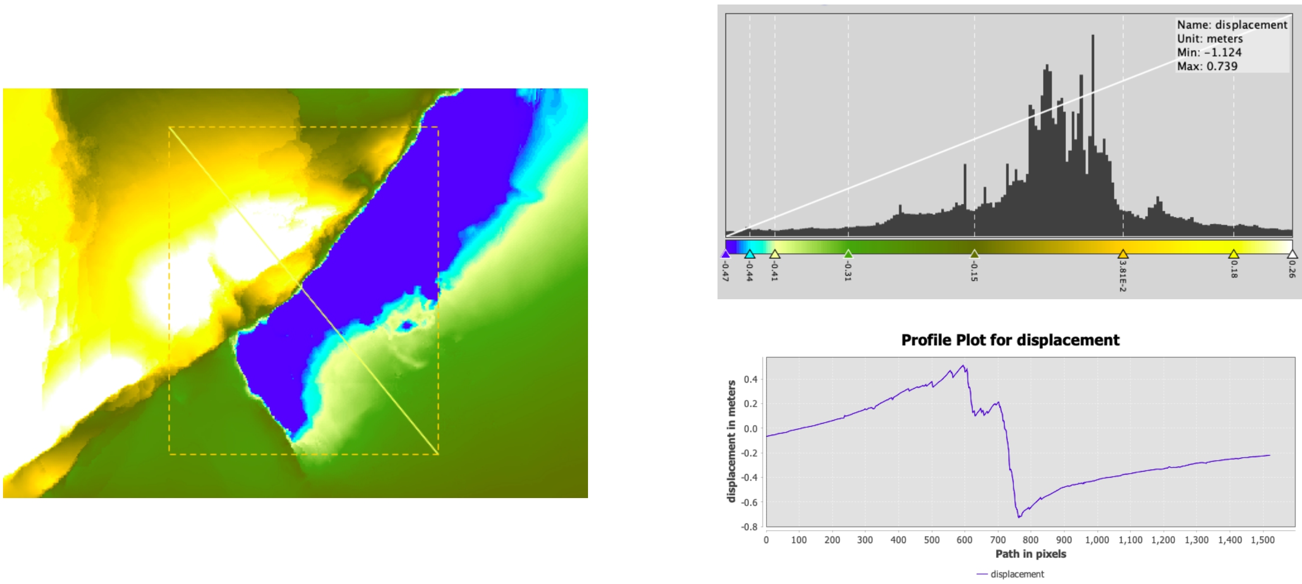

Figure 9

The interferogram and displacement map of an earthquake are rich with information. They provide an efficient method of measurement and offer an opportunity to deeper understand the fault mechanics and effect of earthquakes.

References

[1] ESA (no date) *TOPS Interferometry Tutorial*. Available at: https://step.esa.int/docs/tutorials/S1TBX%20TOPSAR%20Interferometry%20with%20Sentinel-1%20Tutorial_v2.pdf (Accessed: 16 December 2025).

[2] ESA (no date) *Multilook Operator*. Available at: https://step.esa.int/main/wp-content/help/versions/13.0.0/snap-toolboxes/eu.esa.microwavetbx.sar.op.sar.processing.ui/operators/MultilookOp.html (Accessed: 16 December 2025).

[3] Copernicus (no date) *Sentinel-1 Products*. Available at: https://sentiwiki.copernicus.eu/web/s1-products (Accessed: 16 December 2025).

[4] Copernicus (no date) *Sentinel-1 Documentation*. Available at: https://documentation.dataspace.copernicus.eu/Data/SentinelMissions/Sentinel1.html (Accessed: 16 December 2025).

[5] Wikipedia (2025) *2019 Ridgecrest earthquakes*. Available at: https://en.wikipedia.org/wiki/2019_Ridgecrest_earthquakes (Accessed: 16 December 2025).

[6] Xu, X., Sandwell, D.T. and Smith-Konter, B. (2020) Coseismic displacements and surface fractures from Sentinel-1 InSAR: 2019 Ridgecrest earthquakes. *Seismological Research Letters* doi: https://doi.org/10.1785/0220190275.

A Processing Steps and Parameters

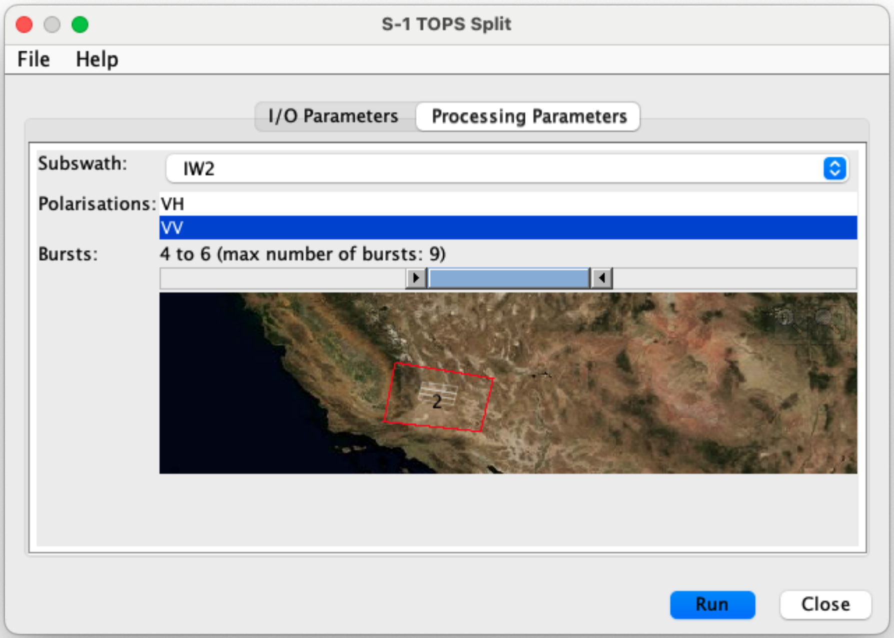

Figure 10: S-1 TOPS Split interface showing subswath and burst selection.

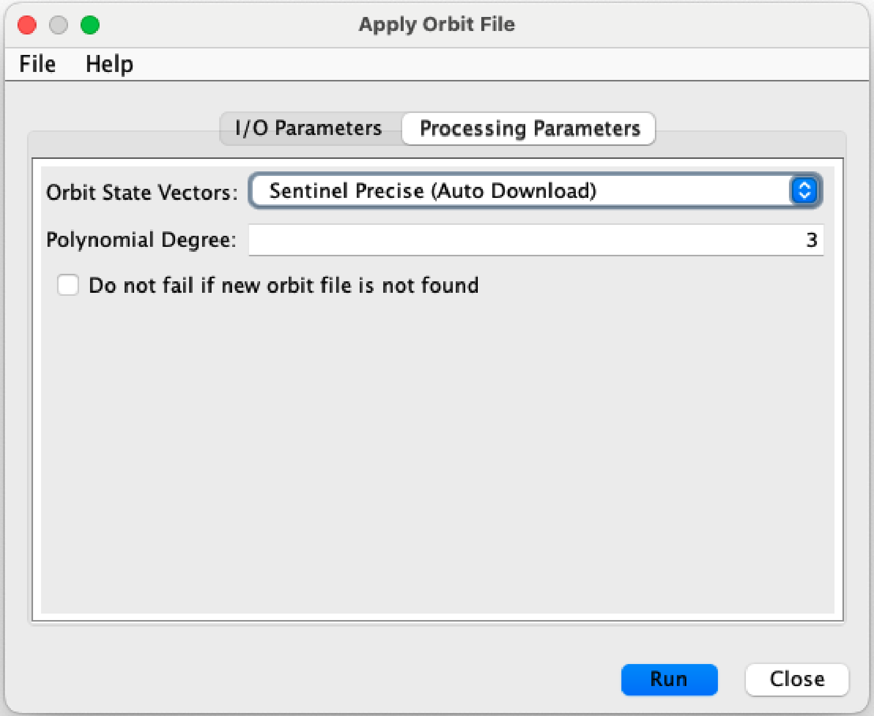

Figure 11: Apply Orbit File interface for POD correction.

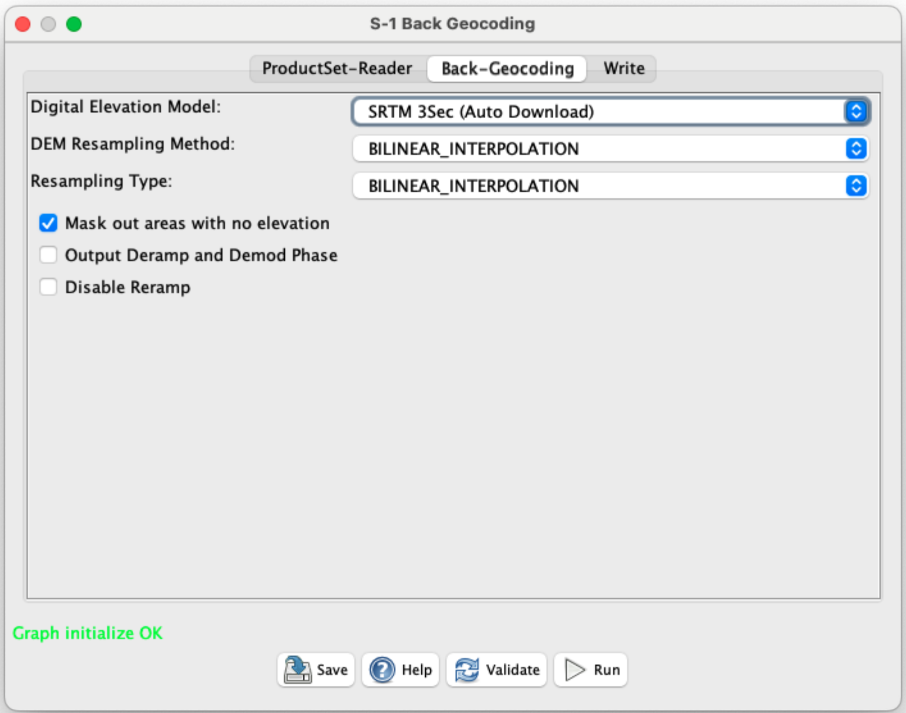

Figure 12: S-1 Back-Geocoding interface for coregistration.

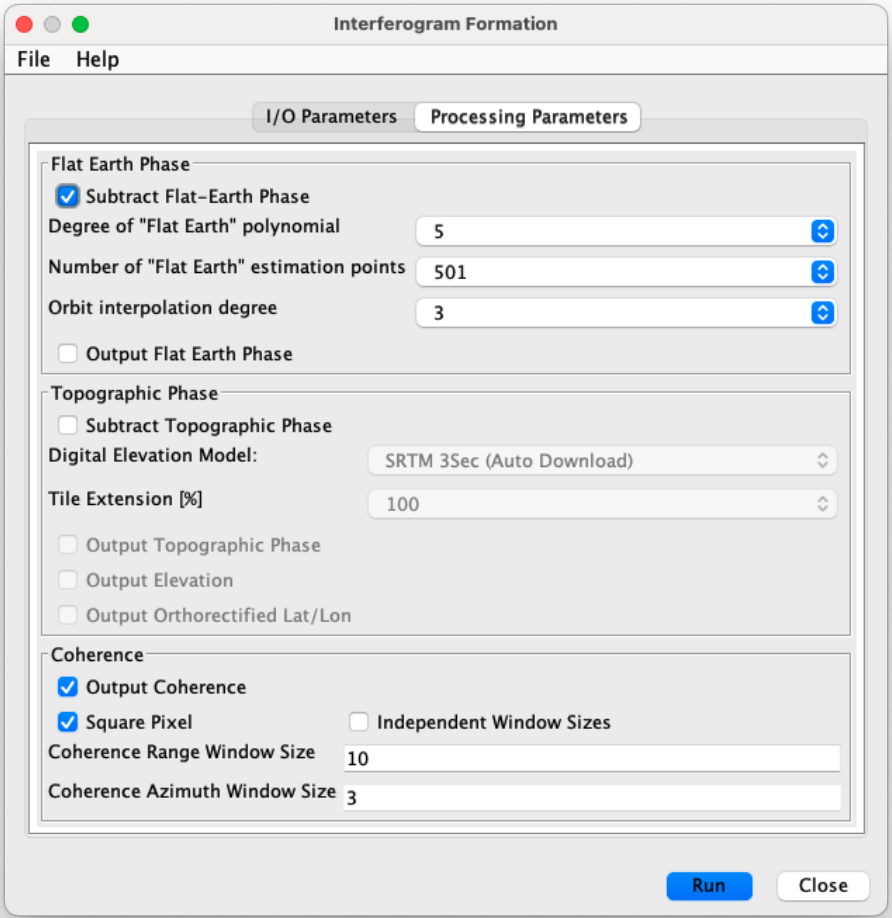

Figure 13: Interferogram Formation interface.

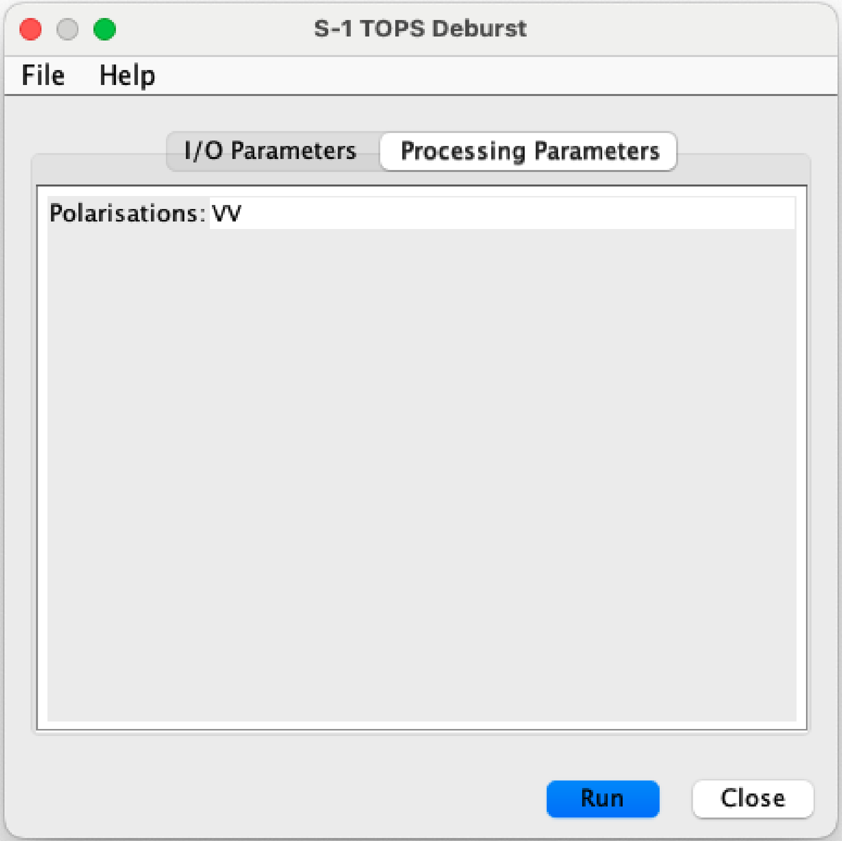

Figure 14: TOPSAR Deburst interface for removing burst boundaries.

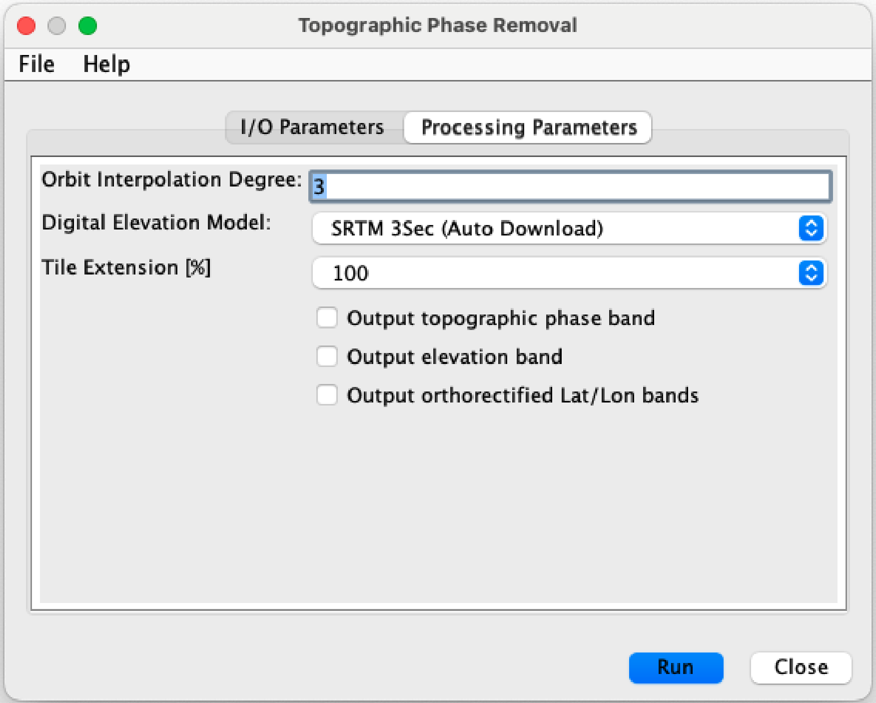

Figure 15: Topographic Phase Removal interface with DEM selection.

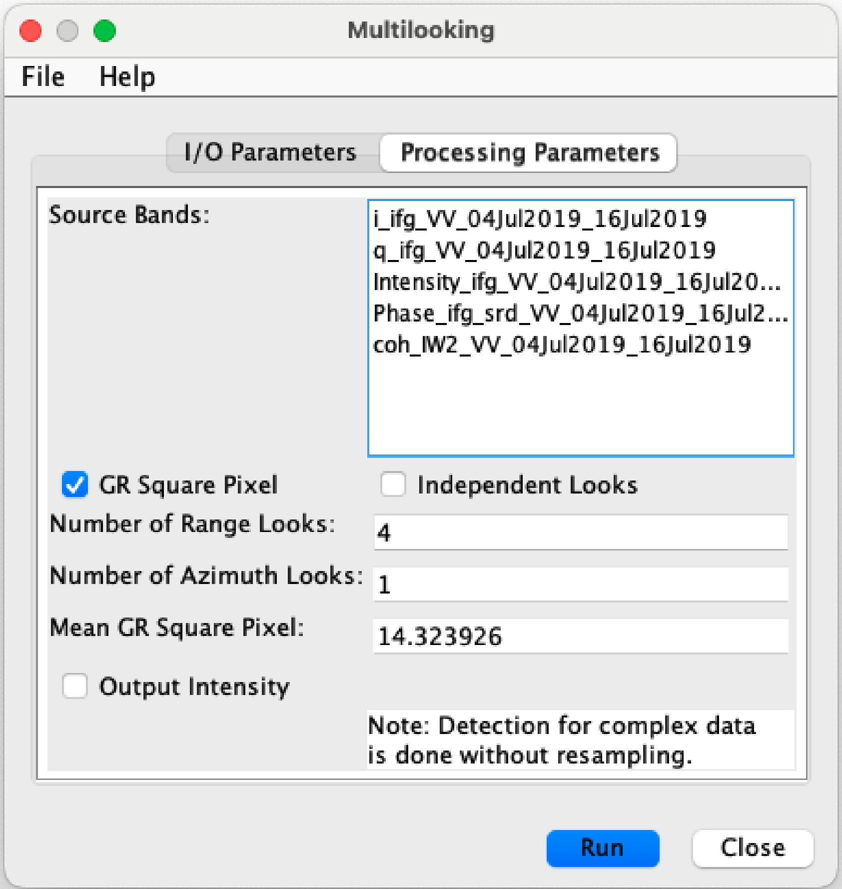

Figure 16: Multilooking interface for noise reduction and pixel squaring.

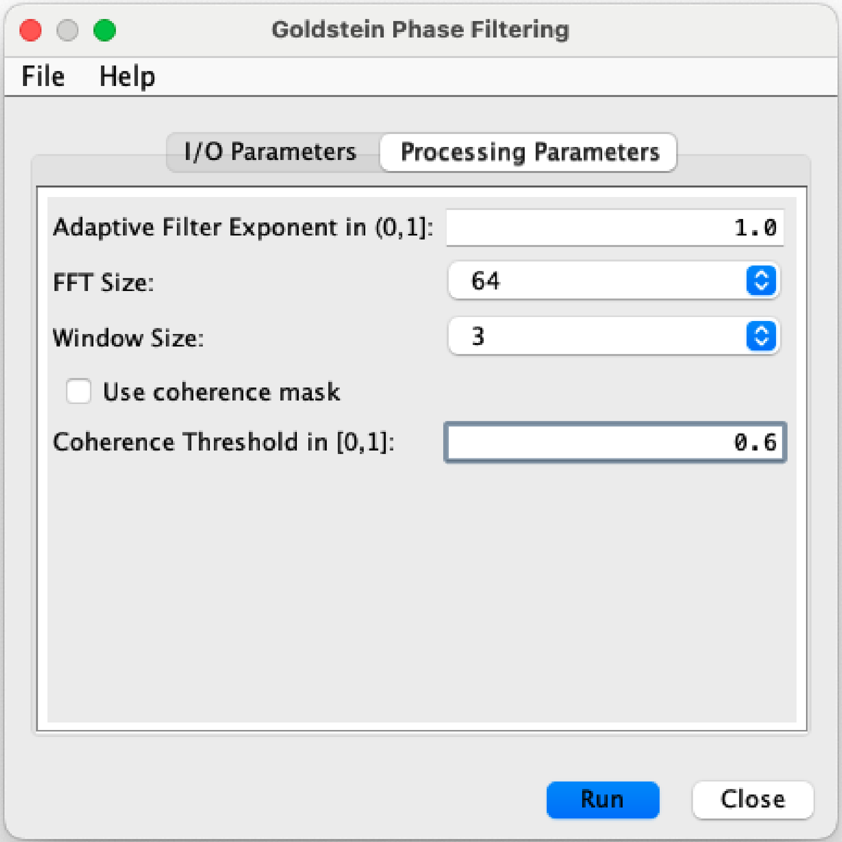

Figure 17: Goldstein Phase Filtering interface.

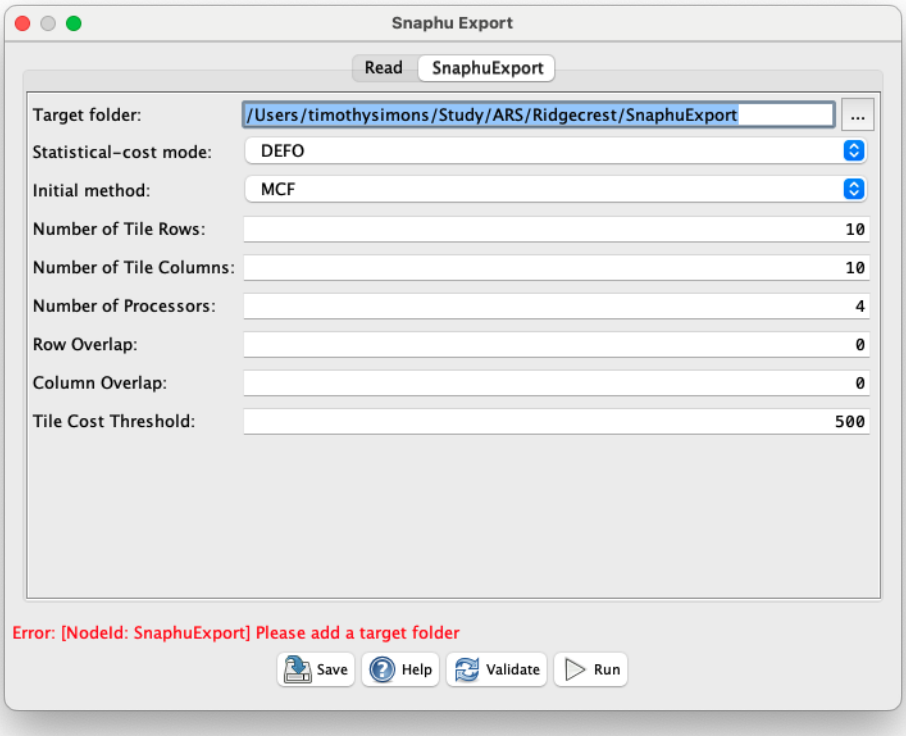

Figure 18: SNAPHU Export interface for phase unwrapping preparation.

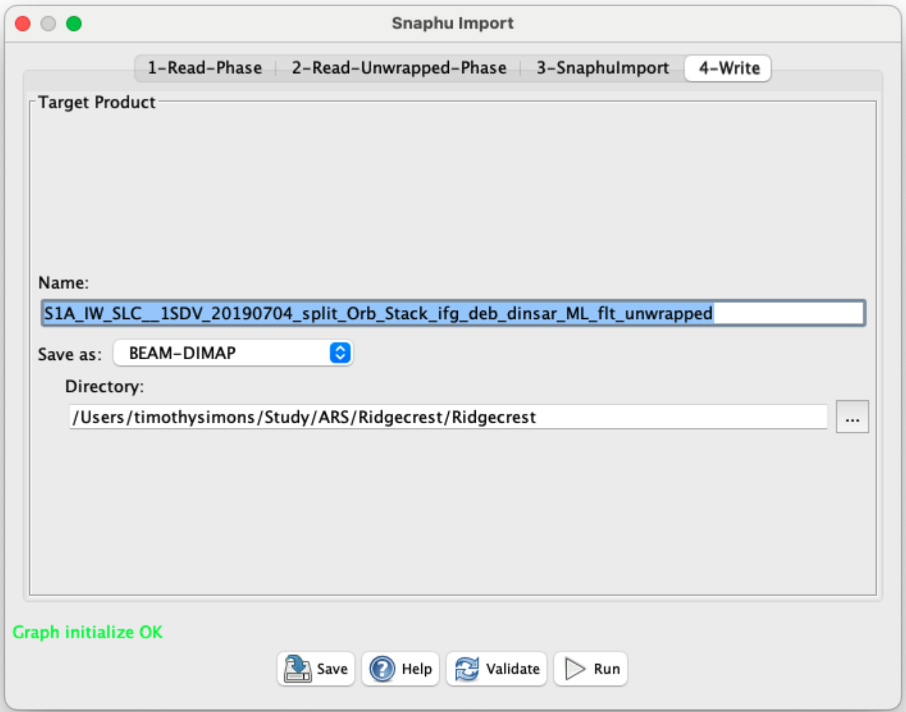

Figure 19: SNAPHU Import interface for unwrapped phase.

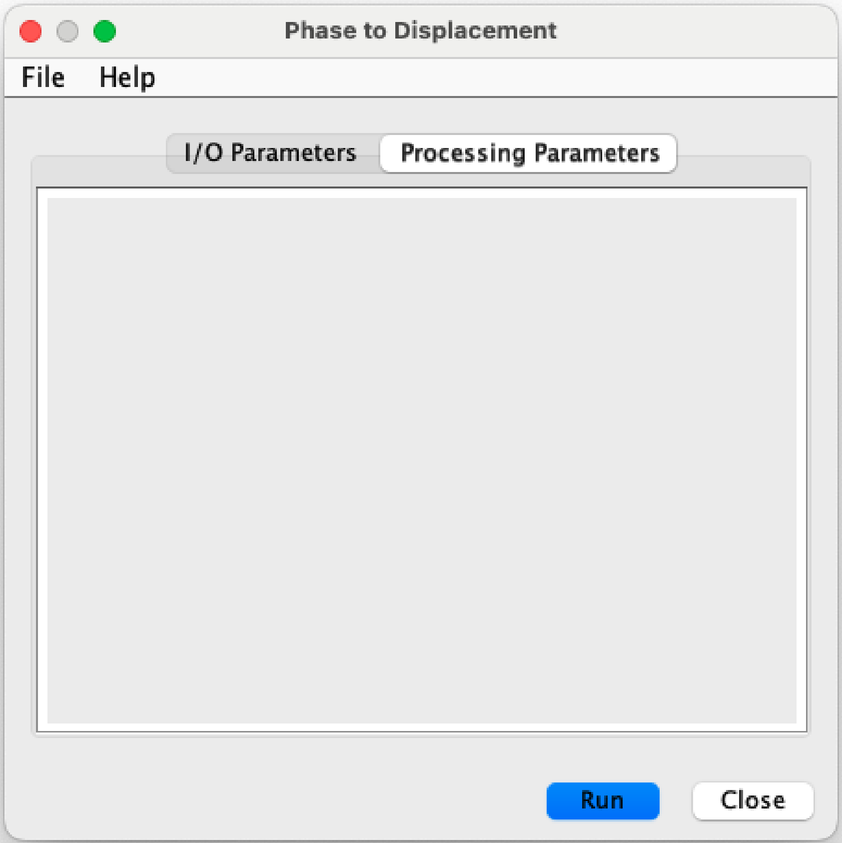

Figure 20: Phase to Displacement interface for displacement map generation.